

LONG LIFE FATIGUE BEHAVIOR OF FILLET WELDED JOINTS UNDER COMPUTER SIMULATED HIGHWAY AND RAILROAD LOADING

By Chitoshi MIKI, Jun MURAKOSHI**, Yukihiro TOYODA***
 and Masahiro SAKANO*****

Fatigue behavior of fillet welded joints with a scallop under highway and railroad loading was studied. Variable amplitude stress fluctuations were generated by computer simulations of highway and railroad live loads. Fatigue failure occurred even if the equivalent stress range was less than the constant amplitude fatigue limit. Therefore, fatigue life evaluation assuming that stress ranges below the fatigue limit did no damage was unconservative. It was verified that the fatigue life under variable amplitude loading could be estimated accurately by applying the fracture mechanics approach with the linear damage rule.

Keywords: fatigue test, fillet weld, variable loading, computer simulation.

1. INTRODUCTION

In steel bridge members, extremely complicated stress fluctuations are induced when trucks or trains are crossing the bridge. Actual stress measurements¹⁾⁻³⁾ indicate that most of stress range components of those stress fluctuations are below the constant amplitude fatigue limit of each structural detail. Therefore, it is of great importance to study the fatigue behavior in a lower-stress and longer-life region under such variable stresses in order to evaluate the fatigue resistance of steel bridge members.

In the fatigue design of railroad bridges in Japan⁴⁾, the modified Miner's rule which disregards the fatigue limit is applied to evaluate the fatigue life under variable stress fluctuations. However, this method is too conservative for most of bridge details because of overestimation of the fatigue damage by lower stress components. Both in BS 5 400⁵⁾ and ECCS Recommendations⁶⁾, Miner's rule is used but the slopes and the cut-off limits of design curves are changed at the specific stress cycles for variable amplitude loads.

A few studies have been carried out in the past regarding the fatigue strength of welded joints subjected to variable amplitude loading with most stress cycles below the constant amplitude fatigue limit. Albrecht and Friedland⁷⁾, Tilly and Nunn⁸⁾ and Fisher et al⁹⁾ indicated that fatigue cracks developed even though the equivalent stress range was well below the constant amplitude fatigue limit. The stress range components of variable stress fluctuations which are greater than the fatigue limit or the fatigue crack growth

* Member of JSCE, Dr. Eng., Associate Professor, Department of Civil Engineering, Tokyo Institute of Technology (O-okayama, Meguro-ku, Tokyo)

** Member of JSCE, M. Eng., Public Work Research Institute, Ministry of Construction (Tsukuba-shi, Ibaragi)

*** Member of JSCE, M. Eng., Electric Power Central Research Institute (Abiko-shi, Chiba)

**** Member of JSCE, Dr. Eng., Research Associate, Department of Construction Engineering, Gunma University (Kiryu-shi, Gunma)

threshold ΔK_{th} may cause fatigue crack propagation, and the percentage of those stress range components may increase with the growth of the fatigue crack. Therefore, the fatigue behavior varies with applied stress fluctuations and structural details. Consequently, it is necessary to carry out fatigue tests using variable amplitude stresses which are as similar to actual stresses as possible.

In order to investigate the fatigue behavior of bridge details in lower-stress and longer-life region, non-load-carrying fillet-welded cruciform joints were tested under computer simulated variable amplitude loading for highway and railroad bridges. In a previous study¹⁰⁾, the authors conducted fatigue crack propagation tests under simulated variable amplitude loading for highway bridge and indicated that the fatigue crack growth threshold ΔK_{th} existed also under variable amplitude loading and that the fatigue crack growth rate could be accurately estimated using ΔK_{th} and the linear cumulative damage rule. The applicability of this result for the fatigue life prediction of welded joints was also examined in this study.

2. METHOD OF TESTING

(1) Specimens

The configurations and dimensions of the non-load-carrying fillet-welded cruciform-type specimen are shown in Fig. 1. This specimen is modeled on the welded connection at the end of the vertical stiffener in a plate girder or at the corner of the diaphragm in a box section member. Simulating a web-to-flange weld or a box corner weld, the longitudinal weld is beaded on along the centerline of the specimen to introduce high tensile residual stresses. A scallop is prepared at the intersection of the welding lines, where weldments are turned round.

The tested steel is SM58 as used in the previous work¹⁰⁾. Mechanical properties and chemical compositions are given in Table 1.

(2) Simulated variable amplitude stresses

Variable amplitude stress waveforms used in fatigue tests and fatigue life analyses are generated by computer simulations¹¹⁾ of live loads on highway or railway bridges. Highway live loads are simulated with the constitution of five types of vehicles given in Table 2, which approximate the traffic flow constituted for the most part by heavy trucks as used in the previous study¹⁰⁾. Railroad live loads are simulated by supposing Shinkansen (Bullet Train System) passenger trains with axle weights defined by a log-normal distribution (maximum : 19 tf, minimum : 16 tf, mean : 17 tf) run in succession⁹⁾. Stress fluctuations are obtained as the bending moment response at the middle of a 20-m span of the simply supported beam, when those columns of live loads are crossing.

Examples of variable amplitude stress waveforms used in highway and railroad loading tests and the non-dimensional stress range spectra counted by the rainflow method are shown in Fig. 2 and Fig. 3, respectively. As to variable stresses for highway loading, the stress fluctuations below the 40 percent of the maximum stress range are deleted for the purpose of saving the time required for fatigue tests. The arrows in Fig. 3 represent the relative equivalent stress ranges as the root-mean-cube values. Those variable amplitude stress spectra well express the characteristics of having an extremely high frequency of lower stress ranges for highway live loading and a relatively narrow band of stress ranges for railroad live loading.

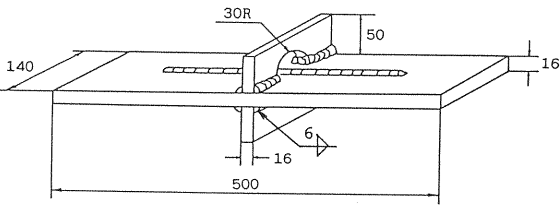


Fig. 1 Specimen (Dimension : mm).

Table 1 Mechanical Properties and Chemical Compositions of SM 58 Steel.

Mechanical properties			Chemical compositions				
yield strength (MPa)	tensile strength (MPa)	elongation (%)	C	Si	Mn	P	S
			x100(%)			x1000(%)	
640	690	34	8	24	166	20	4

Table 2 Traffic Model Constitution for
Highway Live Load Simulation.

Vehicle type	Percentage
Car	10
Small truck	5
2 axes large truck	25
3 axes large truck	50
4 axes trailer	10

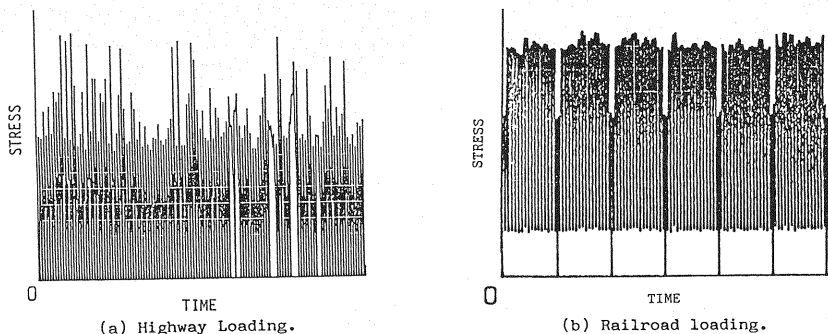


Fig.2 Simulated Variable Stress Fluctuations.

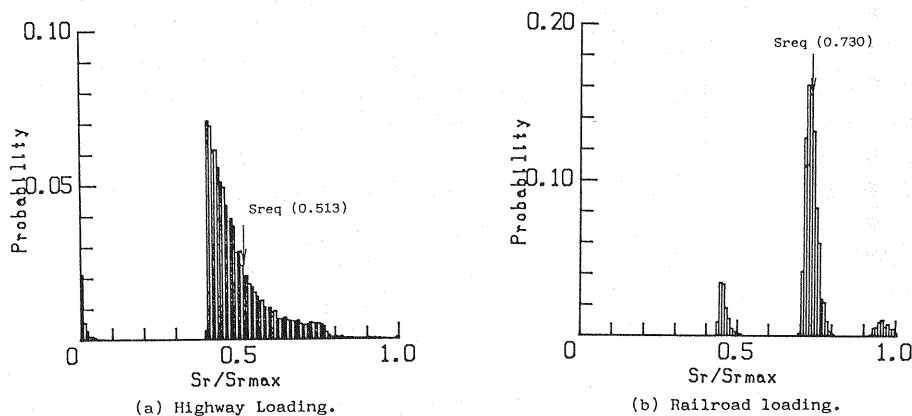


Fig.3 Stress Range Spectra.

(3) Fatigue tests

Fatigue tests were conducted under tensile cyclic loading by an electro-hydraulic fatigue testing machine with a dynamic capacity of 490 kN. The minimum stress value was 13 MPa, and the rate of stress repetition was 10 to 20 Hz. The loading waveform was supplied as the voltage fluctuation which was transformed by a D/A converter from a series of the peak values generated by the computer simulation. Variable amplitude fatigue loading tests were performed under such stress conditions as cross over the fatigue limit obtained by constant amplitude fatigue loading tests.

3. TEST RESULTS AND CONSIDERATIONS

(1) Fatigue life under constant amplitude loading

The relationship between the stress range S_r and the number of stress cycles to failure N_f of each specimen under constant amplitude fatigue loading is shown in Fig. 4. Fatigue cracks started from the toe of the weldment at the re-starting point of turn-round welding (see Fig. 5). The solid line and the broken

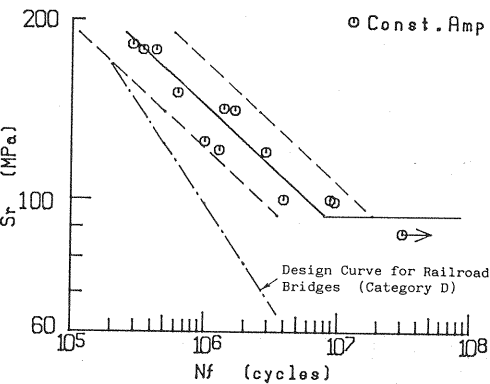


Fig. 4 S_r - N_f Relationships under Constant Amplitude Loading.

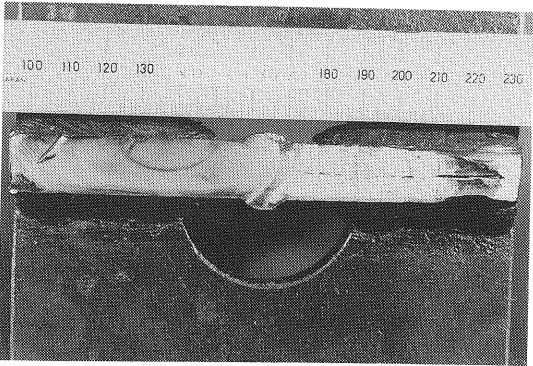


Fig. 5 Failure Surface.

lines in Fig. 4 indicate the mean regression line and mean $\pm 2\sigma$ (σ : standard deviation) lines obtained by the least square method.

$S_r^{4.89} \cdot N_f = 3.56 \times 10^{16} \dots \dots \dots (1)$
 $\sigma = 0.178$

The dashed-dotted line in Fig. 4 is the design curve for the category D of the design standard of steel railroad bridges⁴⁾. The fatigue strength of every specimen is greater than the allowable stress range.

In cases where the stress range S_r is more than 100 MPa, all specimens failed at the number of stress cycles N less than 10 million. When S_r equals to 90 MPa, the specimen did not fail although N exceeds 30 million, and no cracks were detected when inspected by the magnetic particle examination. Consequently, the fatigue limit of the specimen under constant amplitude loading could be defined as being 95 MPa.

(2) Fatigue life under variable amplitude loading

The results of variable amplitude fatigue loading tests are given in Table 3 and shown in Fig. 6. In Table 3, the percentages of stress ranges above the constant amplitude fatigue limit among the whole of variable amplitude stress cycles are 12 to 42 for highway bridge loading and 7 to 88 for railroad bridge loading. The ordinate in Fig. 6 gives the equivalent stress range S_{req} as the root mean m -th ($(\sum_{i=1}^N S_{ri}^m / N)^{1/m}$) of all stress ranges in variable amplitude stresses (see Fig. 7). The m is equal to 4.89 of the power index from the regression line under constant amplitude loading (Eq. (1)). As shown in Fig. 6, the fatigue

Table 3 Results of Variable Amplitude Loading Tests.

Specimen Number	S _{rmax}	S _{req} (MPa)	S _{req} *	N _f (10 ³ cycles)	N _f *	γ (%)
(a) Highway Loading						
1	194	104	117	7200	3040	42.2
2	177	95	115	6410	1680	26.2
3	158	85	110	14400	2170	15.1
4	156	84	109	6260	880	14.1
5	150	81	107	27000	3130	11.6
(b) Railroad Loading						
6	130	97	110	9850	7000	71.1
7	125	93	103	9330	2450	26.2
8	149	111	113	5070	4470	88.2
9	119	88	111	5030	368	7.3
10	121	90	110	6200	589	9.5

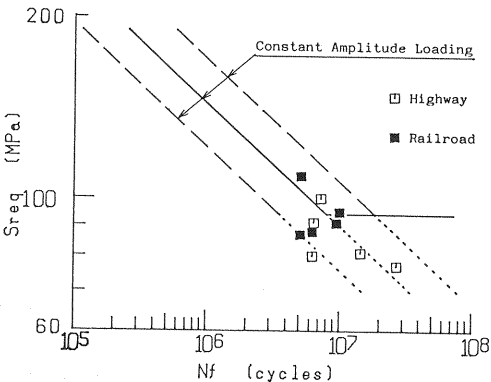


Fig. 6 S_{req} - N_f Relationships under Variable Amplitude Loading.

S_{req} * : Equivalent value of stress ranges above the constant amplitude fatigue limit.
 N_f * : Number of stress cycles above the constant amplitude fatigue limit.
 γ : Percentage of stress cycles above the constant amplitude fatigue limit.

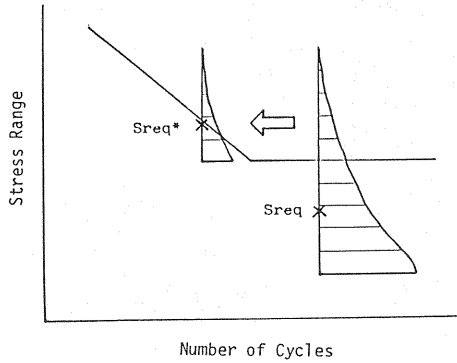


Fig. 7 Evaluation of Fatigue Life by Miner's rule.

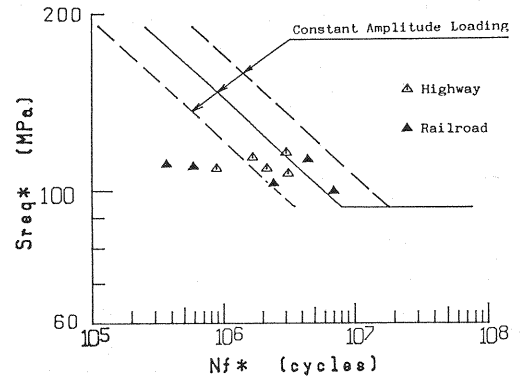


Fig. 8 $S_{req}^*-N_f^*$ Relationships under Variable Amplitude Loading.

failure occurs even when S_{req} is lower than the constant amplitude fatigue limit under both highway and railroad variable amplitude loading. N_f corresponds to the equivalent stress range for the assessment of fatigue life using the modified Miner's rule. The relationship between S_{req} and N_f under both types of variable amplitude loading can be represented by the extension of the 95 percent confidence limit under constant amplitude loading. However, in respect of results under highway variable amplitude loading, stress components lower than the 40 percent of the maximum stress in the stress fluctuation produced by the computer simulation were deleted in fatigue testings. Therefore, the application of the modified Miner's rule to such conditions of variable amplitude stresses provides a suitable estimate of fatigue life. In contrast, fatigue crack propagation tests under similar variable amplitude loading reported by the authors¹⁰⁾ indicate that fatigue crack growth rates obtained on the assumption that all stress cycles including even the lowest stress ranges are effective in fatigue crack growth are overestimated. Consequently, under variable amplitude stresses including stress cycles still lower than the deleting level in these tests, the estimation of fatigue life using the modified Miner's rule may be too conservative.

Fig. 8 shows the variable amplitude fatigue test results rearranged on the assumption that only stress cycles larger than the constant amplitude fatigue limit can initiate fatigue damage. S_{req}^* is the root mean m -th of the stress ranges above the constant amplitude fatigue limit obtained by the method illustrated in Fig. 7, which corresponds to the equivalent stress range for fatigue life assessment applying Miner's rule. The power index m is equal to 4.89 similar to m of S_{req} . N_f^* is the number of stress cycles above the constant amplitude fatigue limit required to bring about the failure of specimens. The S_{req}^* to N_f^* relationships of the specimens are located in the shorter life region of the regression line under constant amplitude loading, so that the fatigue life estimate applying Miner's rule on the basis of the constant amplitude S_r - N_f relationship and the fatigue limit is unsafe under both highway and railroad variable amplitude loading.

4. FATIGUE LIFE ESTIMATION BY FRACTURE MECHANICS CONCEPT

(1) Procedures of analyses

The authors reported in the previous study¹⁰⁾ that the fatigue crack growth rate under variable amplitude loading could be accurately estimated by using the linear damage rule and assuming the stress intensity factor range ΔK higher than the threshold value ΔK_{th} to be effective for crack propagation. In this study, the fatigue life N_f of the specimen, regarded as the fatigue crack propagation life N_p , is estimated applying the fracture mechanics approach¹²⁾. The stress intensity factor range ΔK for each stress cycle is calculated by Eq. (2).

$$\Delta K = F_e \cdot F_s \cdot F_t \cdot F_g \cdot S_r \sqrt{\pi a} \dots \dots \dots (2)$$

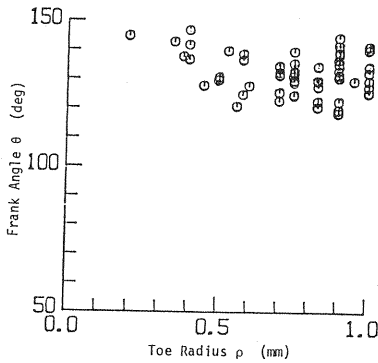


Fig.9 Measured θ and ρ .

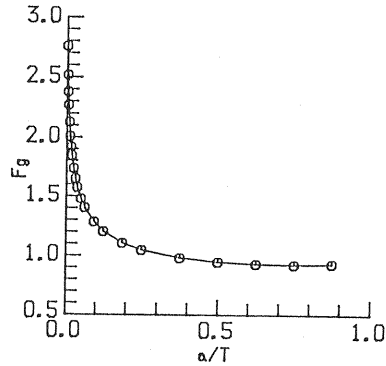


Fig.10 Relationship between F_g and a/T .

where, S_r is nominal stress range on the minimum area, a is crack depth, F_e , F_s , F_t and F_g are correction factors to account for the effects of crack shape, free surface, finite thickness and stress concentration, respectively. In these analyses, because of the assumption of semi-circular surface cracks, $F_e=2/\pi$, $F_s=1$, and F_t is defined by Eq. (3)¹².

$$F_t=(1-0.025\lambda^2+0.06\lambda^4)\sqrt{\sec(\pi\lambda/2)} \dots\dots\dots (3)$$

where, $\lambda=a/T$ (T is the thickness of the specimen). F_g is calculated from the stress intensity factor for an edge crack in a semi-infinite plane subjected to the stress distribution occurred without the crack. The stress distribution is obtained by the finite element analysis with the flank angle θ of 135° and the toe radius ρ of 0.75 mm which are the mean values from the measurements of specimens (see Fig.9). The relationship between F_g and a/T is shown in Fig.10.

The crack growth rate da/dN is defined by Eq. (4) obtained from the constant amplitude fatigue crack propagation tests using the same material¹⁰.

$$da/dN=\left\{ \begin{array}{ll} C\cdot\Delta K^n & (\Delta K>\Delta K_{th}) \\ 0 & (\Delta K\leq\Delta K_{th}) \end{array} \right\} \dots\dots\dots (4)$$

where, $C=1.03\times10^{-8}$, $n=3.0$, $\Delta K_{th}=2.1\text{ MPa}\sqrt{m}$. The crack propagation life N_p is calculated by Eq. (5).

$$N_p=\int_{a_i}^{a_f} da/(C\cdot\Delta K^n) \dots\dots\dots (5)$$

N_p is known to be affected seriously by the initial crack size a_i . In the fatigue life estimation under variable amplitude loading, a_i is defined so that the estimated fatigue life corresponds with the experimental value under constant amplitude loading. The final crack size a_f , conversely, is known to have such little influence on the estimated fatigue life, that it is defined to be 80 percent of the plate thickness.

(2) Results of analyses

The estimated fatigue life under constant amplitude loading is compared with the fatigue test results in Fig. 11. As shown in the figure, the slanting lines of estimated fatigue life curves for $a_i=0.05$, 0.07, 0.1, and 0.2 mm are little different from each other and are analogous to the test results irrespective of a_i . In the case of the horizontal lines of estimated curves, however, the line for $a_i=0.07$ mm corresponds to the test results better than the others.

Fig.12 shows estimated fatigue life curves and test results under variable amplitude loading. $S_{req}-N_f$ curves in the figure were estimated with a_i of 0.07 mm. A solid line denotes highway variable amplitude loading, and the broken line shows the railroad variable amplitude loading. Each of the curves gives a good estimation on the slightly conservative side. Consequently, it has been verified that fatigue life under variable amplitude loading can be estimated accurately by applying the fracture mechanics approach with the $da/dN-\Delta K$ relationship under constant amplitude loading and the linear cumulative damage rule.

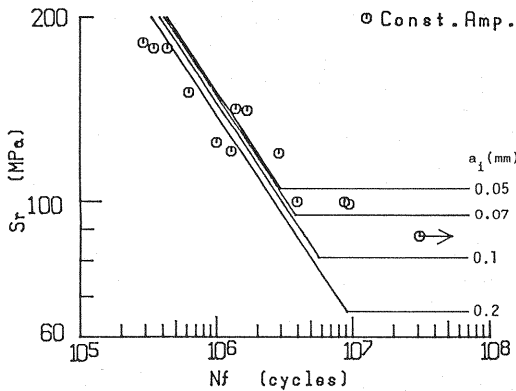


Fig. 11 Estimated S_r - N_f Curves under Constant Amplitude Loading.

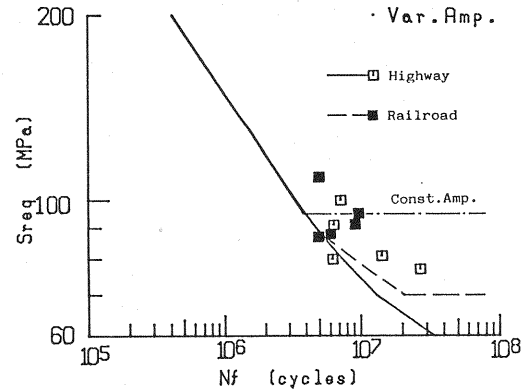


Fig. 12 Estimated S_{req} - N_f Curves under Variable Amplitude Loading.

5. CONCLUSIONS

The long life fatigue characteristics of a typical welded joint in steel bridges under variable amplitude loading which were generated by computer simulations of highway and railroad live loads were studied. The following results were obtained.

(1) Fatigue failure occurs both under highway and railroad variable amplitude loading, even if the equivalent stress range S_{req} calculated from all components of the stress range histogram counted by the rainflow method, is less than the constant amplitude fatigue limit.

(2) The application of the modified Miner's rule provides a suitable estimate of fatigue life under simulated railroad bridge loading and highway bridge loading where stress components lower than the 40 percent of the maximum stress are deleted.

(3) Fatigue life evaluation of highway and railroad bridge members using Miner's rule is unsafe when it is assumed that stress ranges below the constant amplitude fatigue limit do no damage.

(4) Fatigue life under variable amplitude loading could be estimated with sufficient accuracy by applying the linear damage rule and the constant amplitude da/dN - ΔK relationship, considering that only stress components higher than ΔK_{th} contribute to fatigue crack growth.

ACKNOWLEDGEMENTS

The authors would like to thank Dr. Takeshi Mori and Mr. Miyabu Kohno of Tokyo Institute of Technology for their invaluable advice and assistance in carrying out this study.

This study is supported in part by the Grant-in-Aid for General Scientific Research from the Japanese Ministry of Education, Science and Culture ((C) 62550327).

REFERENCES

- 1) Abe, H., Taniguchi, N. and Abe, M. : Fatigue Problem and Repair-Rehabilitation in Railway Bridges, Bridge and Foundation Engineering, Vol. 17, No. 8, pp. 24-29, 1983 (in Japanese).
- 2) Public Works Research Institute : Survey on Technique for Evaluation and Improvement of Durability of Existing Bridges, Technical Notes of PWRI, The Ministry of Construction, No. 2420, 1986 (in Japanese).
- 3) Takenouchi, H., Tanikura, I., Furukawa, M. and Miki, C. : Stress Measurement of Highway Bridges under Actual Traffic Load, Journal of structural Engineering, Vol. 32 A, pp. 631-639, 1986 (in Japanese).
- 4) JSCE : Standard for Design of Steel Railway Bridges, 1983 (in Japanese).
- 5) British Standards Institution : BS 5400, Steel Concrete and Composite Bridges, Part 10. Code of Practice for Fatigue, 1979.
- 6) European Convention for Constructional Steelwork Technical Committee 6 : Recommendations for the Fatigue Design of Steel Structures, Publication No. 43, 1985.

- 7) Albrecht, P. and Friedland, M. : Fatigue-Limit Effect on Variable-Amplitude Fatigue of Stiffeners, Proc. ASCE, Vol. 105, No. ST 12, pp. 2657-2675, Dec. 1979.
- 8) Tilly, G. P. and Nunn, D. E. : Variable Amplitude Fatigue in Relation to Highway Bridges, Proc. Instn Mech Engrs, Vol. 194, pp. 259-267, 1980.
- 9) Fisher, J. W., Mertz, D. R. and Zhong, A. : Steel Bridge Members under Variable Amplitude Long Life Fatigue Loading, National Cooperative Highway Research Program Report 267, Dec. 1983.
- 10) Miki, C., Murakoshi, J. and Sakano, M. : Fatigue Crack Growth in Highway Bridges, Structural Eng./Earthquake Eng., Vol. 4, No. 2, pp. 371-380, Oct. 1987.
- 11) Miki, C., Goto, Y., Yoshida, H. and Mori, T. : Computer Simulation Studies on the Fatigue Load and Fatigue Design of Highway Bridges, Proc. of JSCE, Structural Eng./Earthquake Eng., Vol. 2, No. 1, pp. 13-22, 1985.
- 12) Okamura, H. : Introduction to Linear Fracture Mechanics, Baifukan, 1976 (in Japanese).

(Received May 13 1988)